Electronic Supplementary Information

Material and reagents

All chemical reagents used in this experiment were analytically pure and were not further purified before use. $NiCl_2 \cdot 6H_2O$, $FeCl_3 \cdot 6H_2O$, and *p*-benzoquinone were obtained from Chengdu Kelong Chemical Reagent Factory (Chengdu, China). Terephthalic acid was purchased from Aladdin (Shanghai, China). 3,3',5,5'-tetramethylbenzidine (TMB) was obtained from Sigma-Aldrich (Shanghai, China). Hydrogen peroxide was purchased from Sinopharm Chemical Reagent Co. (Shanghai, China). Ethanol, triethylamine, thiourea (TH), and NaN_3 were purchased by Chongqing Taixin Chemical Co. Ltd. (Beibei, Chongqing). Ultrapure water was used throughout whole trials.

Apparatus

The major apparatuses used in this work were UV-2450 UV-visible spectrophotometer (Suzhou, Shimadzu), PHS-3D precision pH meter (Shanghai Precision Scientific Instrument Co., LTD., China), Type SZCL-B constant temperature heating magnetic stirrer (Zhengzhou Great Wall Science and Trade Co., LTD., China), Type KQ-500DE ultrasonic cleaner (Kunshan Ultrasonic Instrument Co., LTD., China), TGL-20M high-speed table refrigerated centrifuge (Xiangyi, China), JEM 2100 transmission electron microscope (JEOL, Japan, operating voltage 200 kV), Type Hitachi SU8010 scanning electron microscopy (Hitachi, Japan), Renishaw Raman microscope (Renishaw in Via Raman microscope, UK), and ASAP 2020 Micrometeritics instrument (Mike, USA).

Steady-state kinetic of the 2D Ni/Fe MOF

The steady state kinetic assays were carried out for the 2D Ni/Fe MOF, where 0.10 mM H_2O_2 or 0.10 mM TMB was used alternatively at a fixed concentration of one substrate versus varying concentrations of the other one. The Lineweaver−Burk plots by the double reciprocal of the Michaelis−Menten equation (eq. 1) were thus performed to calculate the Michaelis constants (K_m) and the maximal reaction velocity (V_{max}).

$$1/v_o = K_m/V_{max}\,(1/[S]+1/K_m) \qquad (1)$$

Table S1. Contents of C, O, Fe, and Ni elements in the 2D Ni/Fe MOF from EDS analysis.

Element	Atomic (%)
C	64.6
O	29.2
Fe	2.20
Ni	4.00

Table S2. BET specific surface areas, pore volumes, and average pore diameters of the Ni-MOF, Fe-MOF and 2D Ni/Fe MOF.

Samples	Surface area (m^2/g)	Total pore volume (cm^3/g)	Average pore diameter (nm)
Ni-MOF	17.95	0.11	21.7
Fe-MOF	10.68	0.041	/
2D Ni/Fe MOF	75.31	0.19	12.9

Table S3. Catalytic activity difference among different batches of Ni/Fe MOF prepared with the same method.

Batch No.	1	2	3	RSD (%)[a]
Catalytic activity (%)	100	98.0	97.6	1.3

[a] RSD for three batches of Ni/Fe MOF.

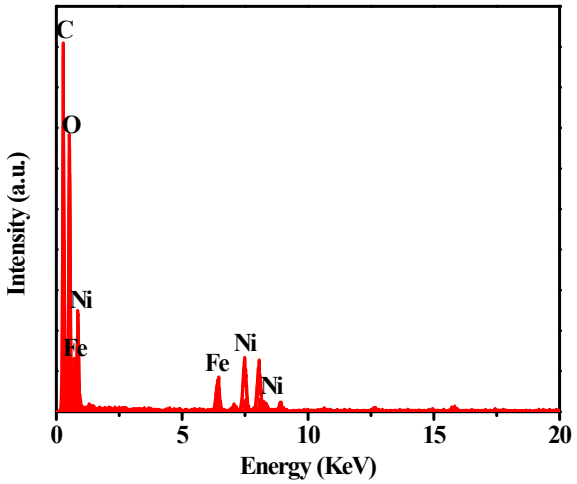

Figure S1. EDS spectrum of the 2D Ni/Fe MOF.

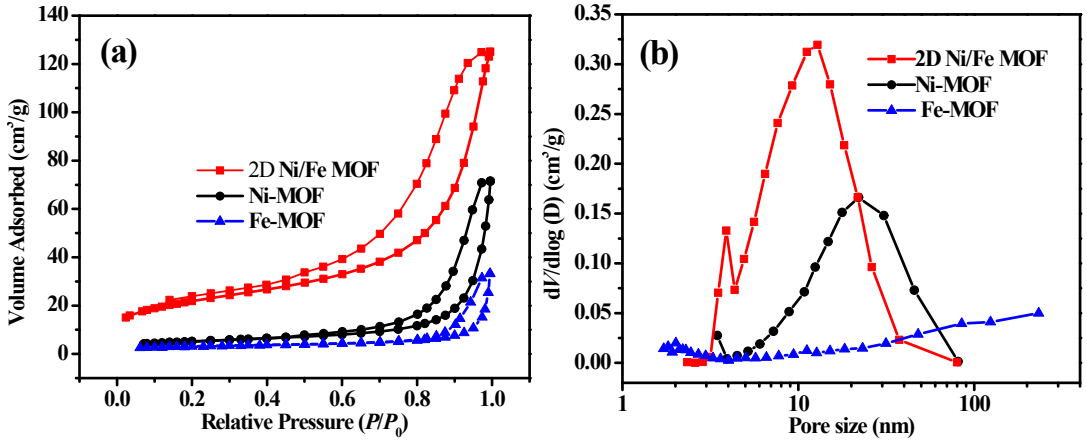

Figure S2. (a) Nitrogen adsorption-desorption isothermal curves of the Ni-MOF, Fe-MOF and 2D Ni/Fe MOF; (b) Pore diameter distribution curves of the Ni-MOF, Fe-MOF and 2D Ni/Fe MOF.

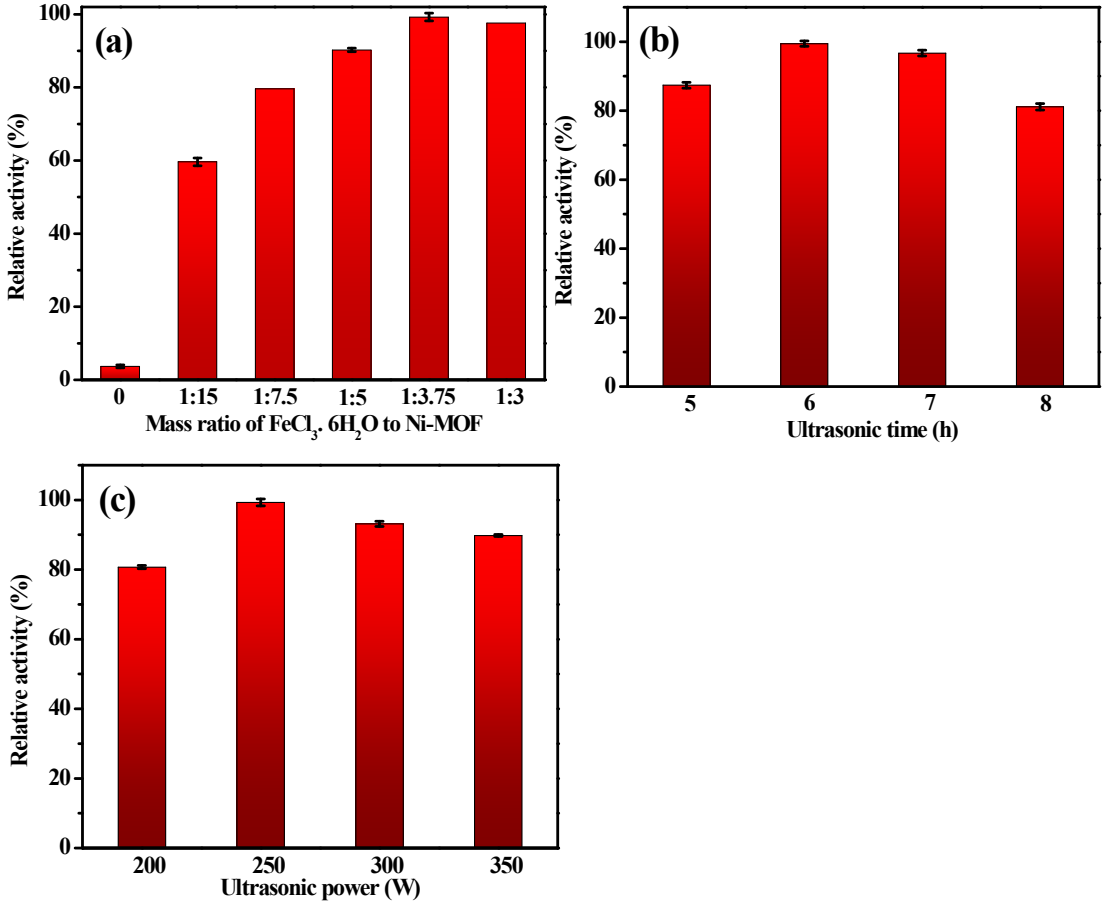

Figure S3. Effects of (a) mass ratio of $FeCl_3 \cdot 6H_2O$ to Ni-MOF, (b) ultrasonic time, and (c) ultrasonic power on the peroxidase-like activities of the resultant product; Conditions: 0.1 mM TMB, 0.1 mM H_2O_2, 20 mg/L catalyst, 25 °C, 15 min, 0.2 M NaAc-HAc buffer (pH 3.0). Error bar shows the standard deviation of three independent measurements.

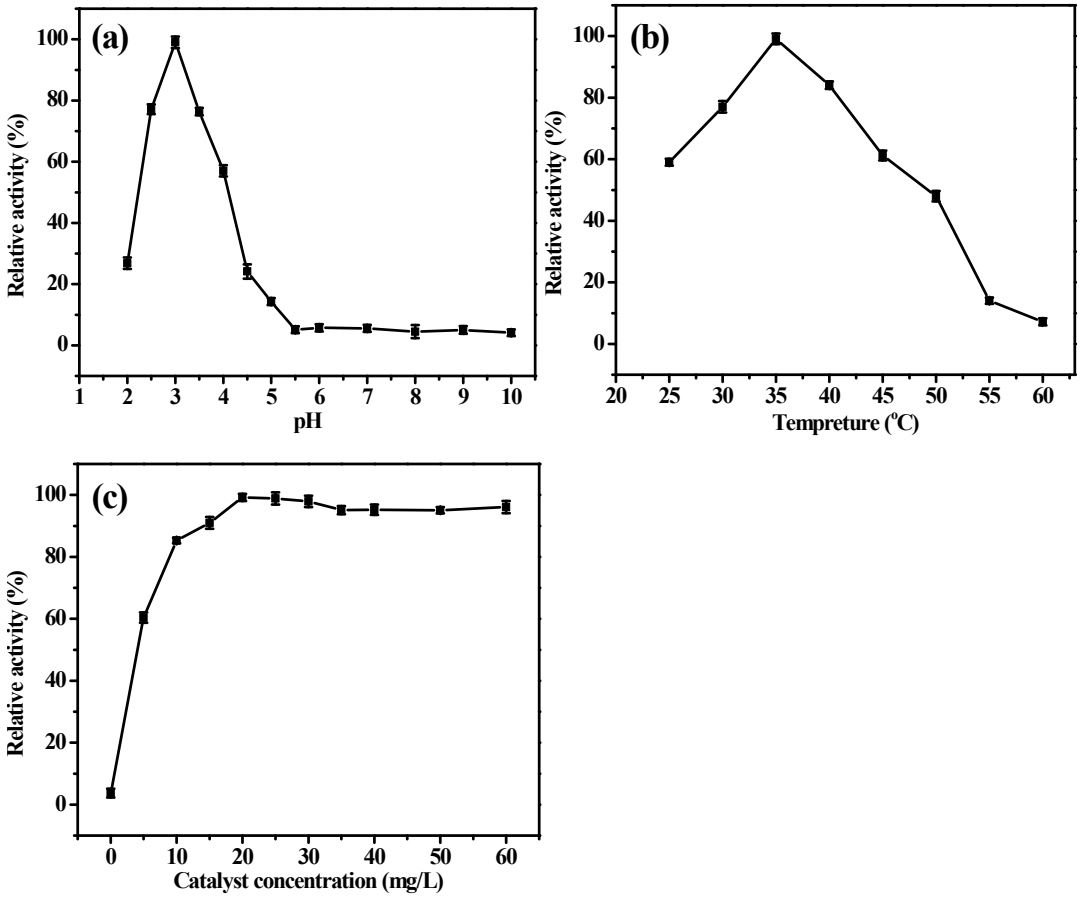

Figure S4. (a) Effect of solution pH value on the peroxidase-like activities of the 2D Ni/Fe MOF. Conditions: 0.1 mM TMB, 0.1 mM H_2O_2, 20 mg/L catalyst, 35 °C, 15 min. (b) Effect of temperature on the peroxidase-like activities of the 2D Ni/Fe MOF. Conditions: 0.1 mM TMB, 0.1 mM H_2O_2, 20 mg/L catalyst, 15 min, 0.2 M NaAc-HAc buffer (pH 3.0). (c) Effect of concentration of 2D Ni/Fe MOF on the peroxidase-like activities of the 2D Ni/Fe MOF. Conditions: 0.1 mM TMB, 0.1 mM H_2O_2, 35 °C, 15 min, 0.2 M NaAc-HAc buffer (pH 3.0). Error bar shows the standard deviation of three independent measurements.

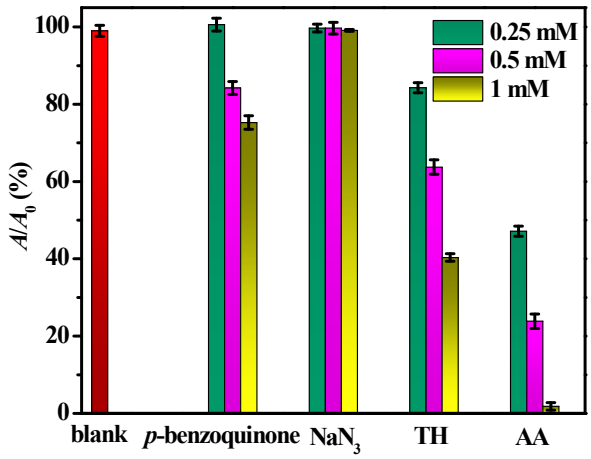

Figure S5. The effects of different reactive oxygen species (ROS) scavengers with varied concentrations on the A/A_0 of the 2D Ni/Fe MOF/TMB/ H_2O_2 system. The A and A_0 are the A_{652} of the 2D Ni/Fe MOF/TMB/H_2O_2 system with and without ROS scavengers, respectively. Reaction conditions: 0.1 mM TMB, 0.1 mM H_2O_2, 20 mg/L catalyst, pH 3.0 acetate buffer (0.2 M), 15 min reaction at 35 °C. Error bar shows the standard deviation of three independent measurements.

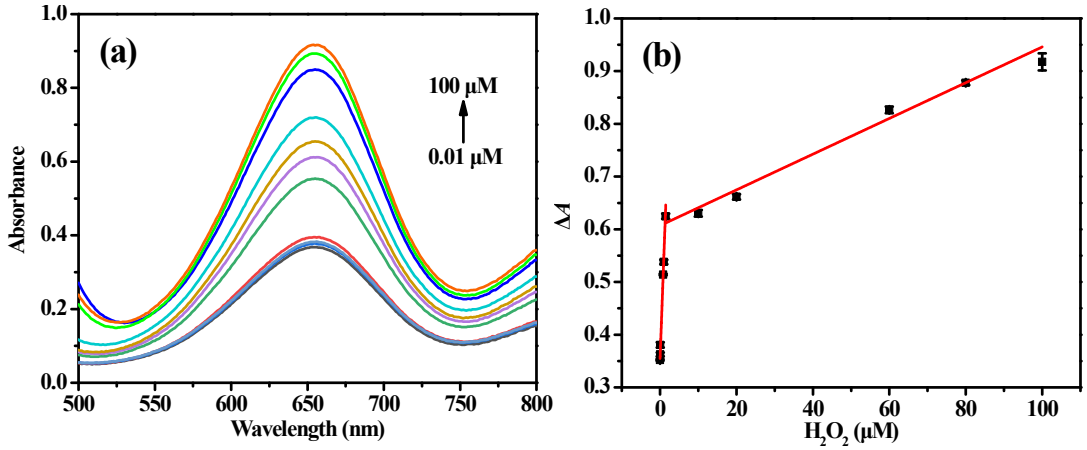

Figure S6. (a) UV-vis spectra and (b) corresponding linear-fitted lines of the 2D Ni/Fe MOF catalyzed TMB oxidation with different concentrations of H_2O_2. Error bar shows the standard deviation of three independent measurements.

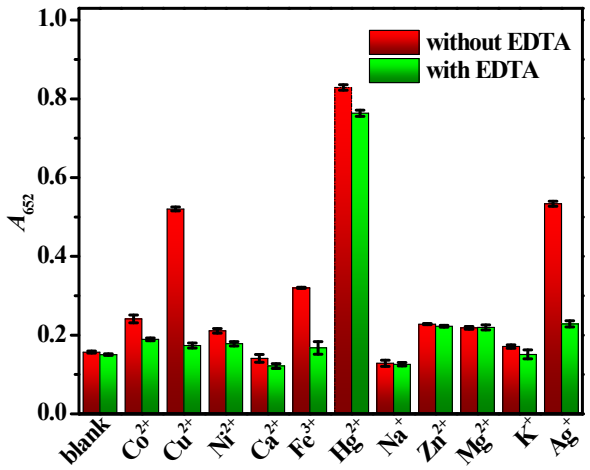

Figure S7. A_{652} of the TMB/H_2O_2/2D Ni/Fe MOF/GSH system in the presence of 100 μM different metal ions with and without 0.5 mM EDTA. Reaction conditions: 0.1 mM TMB, 0.1 mM H_2O_2, 20 mg/L Ni/Fe MOF dispersion, 60 μM GSH, pH 3.0 acetate buffer (0.2 M), 35 °C for 15 min reaction. Error bar shows the standard deviation of three independent measurements.

Table S4. Comparison of analytical performance of the 2D Ni/Fe MOF nanozyme for sensing H_2O_2, GSH, and Hg^{2+} with other materials.

Catalyst	targets	Measurement method	Linear range (μM)	LOD (μM)	Refs
Cu NPs	H_2O_2	Colorimetry	0.15 – 12.5	0.132	[1]
NiFe LDH nanosheet	H_2O_2	Colorimetry	10 – 500	4.4	[2]
NiS nanocubes	H_2O_2	Colorimetry	4 – 40	1.72	[3]
Ru−C_3N_4	H_2O_2	Fluorimetry	0.2 – 1000	0.05	[4]
2D Ni/Fe MOF	H_2O_2	Colorimetry	0.01 – 100	0.01	This work
MnO_2-SiO_2 NPs	GSH	Fluorimetry	0.5 – 100	0.2	[5]
MnO_2 nanosheets	GSH	Colorimetry	1 – 25	0.3	[6]
Fe_3O_4 NPs	GSH	Colorimetry	3 – 30	3	[7]
$Cu_{1.8}S$ NPs	GSH	Colorimetry	500 – 10000	60	[8]
2D Ni/Fe MOF	GSH	Colorimetry	0.02 – 100	0.01	This work
DNA/AuNPs	Hg^{2+}	Colorimetry	0 – 5	0.5	[9]
Ag@GO hybrid	Hg^{2+}	Colorimetry	10 – 200	0.338	[10]
TEA-CdSe QDs	Hg^{2+}	Fluorimetry	0 – 32	0.19	[11]
2D Ni/Fe MOF	Hg^{2+}	Colorimetry	0.1 – 200	0.10	This work

References

1. N. Wang, B. Li, F. Qiao, J. Sun, H. Fan, S. Ai, *J. Mater. Chem. B*, 2015, **3**, 7718−7723.
2. T. Zhan, J. Kang, X. Li, L. Pan, G. Li, W. Hou, *Sens. Actuators B*, 2018, **255**, 2635−2642.
3. H. Liu, H. Ma, H. Xu, J. Wen, Z. Huang, Y. Qiu, K. Fan, D. Li, C. Gu, *Anal. Bioanal. Chem.*, 2019, **411**, 129−137.
4. W. Deng, Y. Peng, H. Yang, Y. Tan, M. Ma, Q. Xie, S. Chen, *ACS Appl. Mater. Interfaces,* 2019*,* **11***,* 29072−29077.
5. X. Zhang, R. Kong, Q. Tan, F. Qu, F. Qu, *Talanta*, 2017, **169**, 1−7.
6. J. Liu, L. Meng, Z. Fei, P. J. Dyson, X. Jing, X. Liu, *Biosens. Bioelectron.*, 2017, **90**, 69−74.
7. Y. Ma, Z. Zhang, C. Ren, G. Liu, X. Chen, *Analys*t, 2012, **137**, 485−489.
8. H. Zou, T. Yang, J. Lan, C. Huang, *Anal. Methods*, 2017, **9**, 841−846.
9. X. Xu, J. Wang, K. Jiao, X. Yang, *Biosens. Bioelectron.*, 2009, **24**, 3153−3158.
10. K. Z. Kamali, A. Pandikumar, S. Jayabal, R. Ramaraj, H. N. Lim, B. H. Ong, C. S. D. Bien, Y. Y. Kee, N. M. Huang, *Microchim. Acta*, 2016, **183**, 369−377.
11. Z. B. Shuang, Y. Wang, W. J. Jin, *Talanta*, 2009, **78**, 364−369.